Advanced Energy Systems and Intelligent Geoscience (AESIG)
https://www.mospbs.com/journal/aesig

• *Article* •

Study of Methane Hydrate Phase Transition and Multiphase Flow Characteristics: Effect of Pressure and Initial Hydrate Saturation

Huiru Sun*

Deep Earth Energy Laboratory, Department of Civil and Environmental Engineering, Monash University, Building 60, Melbourne, VIC 3800, Australia.

***Corresponding Author:** Huiru Sun **Email:** huiru.sun@monash.edu

Received: 05 February 2026 **Accepted:** 13 February 2026

Abstract: Hydrate reservoirs often experience phase transitions such as decomposition and reformation during production process, which can significant fluid flow and reduce gas recovery efficiency. To reveal the mechanism between hydrate phase transition and gas–water two-phase flow behaviors, a visualized experimental setup was developed to monitor hydrate phase transition characteristics under different initial pressure and saturation conditions during the multiphase flow process. The experimental results indicated that initial conditions played a critical role in the onset timing of hydrate decomposition and flow continuity. The high hydrate saturation and pressure were more likely to induce flow blockage and delayed decomposition of methane hydrate. Intermittent "flow–blockage–recovery" dynamics were observed, suggested the repetitive hydrate decomposition–reformation cycles. Moreover, gas–water flow was not only a consequence of phase change but also a driver that promoted local decomposition and flow path reconstruction through thermal and pressure disturbances. This study provided experimental insights into the non-equilibrium interactions between flow and phase transition in hydrate reservoirs and contributed to developing flow-control strategies for efficient hydrate exploitation.

Keywords: Methane hydrate resources; Phase transition characteristic; Multiphase flow; Hydrate saturation; Production pressure

Nonmenclature

Abbreviations	
MH	Methane Hydrate
Symbols	
Shi	Initial Saturation of Methane Hydrate
Vw	Water Flow Rate
Vg	Gas Flow Rate
Pb	Backpressure
Bi	Flow Path Blockage

1 Introduction

Methane hydrate is a typical non-stoichiometric crystalline compound, in which hydrogen-bonded water molecules form cage-like structures that encapsulate small guest gas molecules such as CH_4, CO_2, and N_2 [1-3]. Owing to its widespread occurrence in natural reservoirs,

DOI: https://doi.org/10.58244/aesig.263579

including marine continental margin sediments and permafrost regions, methane hydrate has been recognized as a promising unconventional energy resource. Its enormous reserves, high volumetric energy density, and relatively clean combustion characteristics make it a potential bridge energy for future low-carbon transitions [4-6]. However, methane hydrate exploitation and geological stability are strongly governed by complex multiphase transport processes in porous sediments. During hydrate formation and dissociation, the flow behavior of gas and liquid phases is not only controlled by thermodynamic conditions such as temperature and pressure but is also closely coupled with dynamic hydrate phase transitions. These phase transitions may induce pore-scale blockage, permeability reduction, capillary pressure alteration, and continuous evolution of gas-water interfacial configurations, thereby significantly affecting fluid migration pathways and reservoir-scale transport properties [7, 8].

In recent years, increasing experimental and numerical evidence has highlighted the strong interaction between hydrate phase transitions and gas-water two-phase flow in porous media [9]. Laboratory-scale investigations have demonstrated that hydrate formation preferentially occurs at gas-water interfaces and pore throats, leading to significant reductions in permeability and pronounced flow heterogeneity [10, 11]. In particular, pore-scale visualization techniques such as X-ray CT and MRI have been increasingly employed to directly capture hydrate growth patterns, phase redistribution, and blockage evolution during multiphase transport processes [7, 12, 13]. Beyond pore-scale observations, several studies have reported that hydrate phase transitions can substantially alter capillary pressure and relative permeability relationships, thereby modifying gas–water displacement efficiency and triggering nonlinear flow resistance in hydrate-bearing sediments [14-16]. Such hydrate-induced multiphase flow effects are especially critical under dynamic production conditions, where hydrate dissociation and secondary reformation may coexist, resulting in cyclic permeability evolution and localized sealing behavior [17-19].

To better interpret these complex couplings, various modeling frameworks have been proposed. Christopher et al [20] developed a novel hydrate kinetics and transportability model to characterize the influence of intermittent flow regimes on hydrate formation rates and hydrate slurry transport behavior. Wu et al [21] established a comprehensive computational fluid dynamics-thermo-hydro-chemo coupled model to investigate hydrate phase transition processes during extraction. Their results revealed that rapid hydrate formation preferentially occurred near the pore walls due to local temperature and pressure gradients, leading to water accumulation and flow heterogeneity.

Notably, hydrate phase transitions are often accompanied by significant volumetric changes and solid crystal growth, which can continuously reshape pore structures and modify effective flow pathways [22]. Such feedback mechanisms may trigger nonlinear flow resistance, localized sealing effects, and multiphase redistribution, posing challenges for accurate prediction of reservoir response and safe production control. Therefore, elucidating the coupling mechanisms between hydrate phase transitions and gas-water multiphase flow is of great significance for improving our understanding of hydrate-bearing sediment behavior, optimizing hydrate production strategies, enhancing numerical reservoir simulations, and ensuring long-term engineering safety in hydrate exploitation and CO_2 sequestration scenarios.

2 Experimental section

2.1 Experimental setup and materials

The experimental setup primarily consists of an MRI system, reactor, injection pump, thermostat bath, pressure transducer and data acquisition system. Fig. 1 shows a schematic of the experimental setup, in which the MRI system is used to monitor the variations in water distribution during the MH phase transition process. Th parameters of the MRI system are as follows: echo time (TE) = 4.39 ms, MRI image matrix = 128 × 128 pixels, and the field of view (FOV) = 30 mm × 30 mm (2.0 mm in thickness). The effective size of high-pressure reactor is 15 mm (diameter) × 200 mm (high). Three injection pumps are used to inject gas and deionized water, and to control the backpressure. The temperature of the vessel, injection pumps and MRI system are controlled by three thermostat baths. Two pressure transducers (3510CF, Emerson Electric Co., Ltd., St. Louis, USA) were used to measure the inlet pressure and outlet pressure.

The experimental materials primarily consist of BZ-02 glass beads, high-purity CH_4 gas, and deionized water. The diameter range BZ-02 glass beads are 0.177~0.250 mm. The purity of CH_4 gas is 99.999%. Deionized water, with a conductivity of 0.69 μS/cm, is utilized to saturate the porous media.

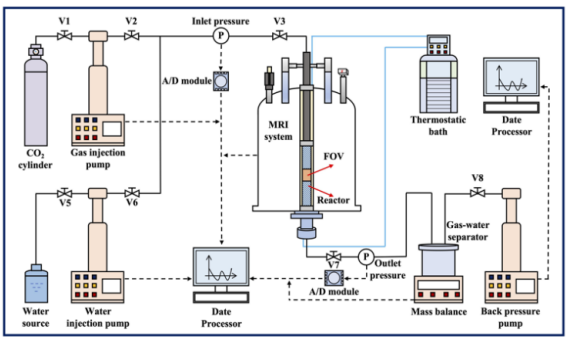

Fig.1 Diagrammatic drawing of the MRI visualization experimental setup

2.2 Experimental procedure

BZ-02 glass beads were tightly packed into the vessel. Next, deionized water was injected into the vessel and then the vessel pressure was pressurized to 6000 kPa to saturate the porous media. When the porous media was considered fully saturated, the high-pressure methane gas was injected to displace partial pore water. Then, the vessel was pressurized to 6000 kPa via methane gas injection and kept constant to form hydrate. The temperature was kept at 274.15 K and kept stable during the whole hydrate formation process. The methane hydrate sediment with different saturation was obtained by controlled the initial pore water amount.

After that, the reactor pressure was adjusted to design value using backpressure pump. Next, the water and gas were simultaneously injected into the reactor at the design flow rate to induce the hydrate phase transition. The temperature of flowing water and gas was maintained at 273.95 K to avoid hydrate decomposition induced by temperature change. During the flow process, when the inlet pressure reached the maximum threshold (15000 kPa), it indicated potential blockage within the flow path. Consequently, the backpressure was gradually decreased until continuous liquid flow was re-established through the hydrate sediment. The experimental results are shown in Table 1.

Table 1 Experimental conditions and parameter

Case	S_{hi} (%)	V_w (mL/min)	V_g (mL/min)	P_b (kPa)	B_i
1	18	10	2	3500	No
2	22			3500	
3	28			6000	Yes

3 results and discussion

To elucidate the coupling mechanism between hydrate phase transitions and gas–water flow behavior, three representative flow scenarios in methane hydrate-bearing sediments were systematically compared. Fig. 2 illustrates the evolution of dynamic water distribution, where brighter regions correspond to higher water content and lower hydrate saturation.

In Case 1, a stable gas-water two-phase flow was maintained throughout the experiment. The continuous expansion of the water-rich zone from inlet to outlet, without any observable interruption, suggests that the ongoing hydrate decomposition was sufficient to prevent channel blockage. No signs of secondary hydrate formation or flow hindrance were detected, and gas-water coexistence was preserved. This case represents a low-saturation, low-pressure regime where hydrate dissociation promotes unobstructed flow. In Case 2, although the system initially exhibited gas-water two-phase flow, a transition to water-dominated flow occurred after approximately 64 mins. This was indicated by a marked increase in water content and the diminishing presence of gas flow signatures. The observed flow shift was primarily caused by insufficient gas replenishment, leading to local water entrapment and the weakening of gas-driven transport. This scenario reflects a condition where moderate hydrate saturation and limited gas availability disrupt the dynamic balance of phase transport. In Case 3, a pronounced flow blockage behavior emerged. Initially, both water and gas flows were severely restricted. However, at around 48 mins, a localized increase in brightness indicated hydrate decomposition, followed by gradual re-establishment of water pathways after 62 mins. This "blockage-reopening" cycle was triggered by the high initial hydrate saturation and flow pressure, which enhanced

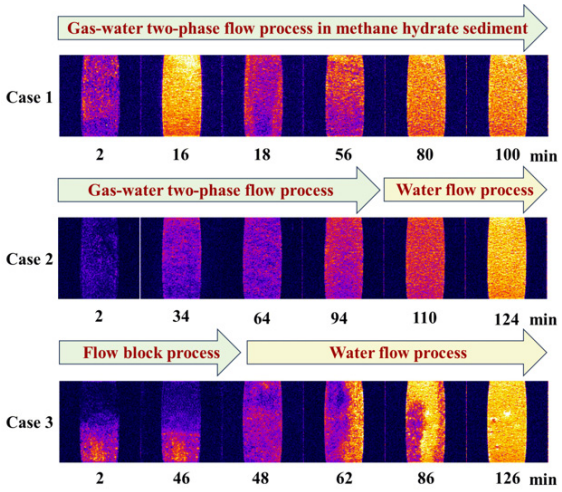

Fig. 2 Variation of MH and water phase distribution in the multiphase flow in Cases 1~3

localized pressure gradients and facilitated abrupt hydrate phase transitions. Among all cases, Case 3 most clearly demonstrated the nonlinear feedback between MH decomposition, fluid redistribution, and transient blockage behavior. These findings suggest that hydrate phase transitions can either facilitate or hinder gas–water flow, depending on the initial thermodynamic and saturation conditions. The results are most applicable to shallow marine hydrate reservoirs under non-isothermal depressurization, where hydrate distribution and pressure gradients play dominant roles in flow regime evolution. However, the observed behaviors may differ in more heterogeneous or clay-rich formations, where capillary forces and sediment structure impose additional constraints.

Fig. 3 illustrates the temporal evolution of water saturation during hydrate phase transitions in Case 1, Case 2, and Case 3. Although all cases ultimately reached near-complete hydrate decomposition, distinct differences were observed in their onset time, progression patterns, and dynamic stability, reflecting the strong coupling between phase transitions and local flow regimes.

In Case 1, hydrate decomposition initiated

early and progressed continuously, as indicated by a steady increase in water saturation. This behavior suggests that hydrate dissociation was primarily governed by pressure-driven decomposition under well-connected flow channels. The persistent gas-water two-phase flow maintained sufficient mass and heat transfer conditions, preventing secondary hydrate formation and enabling efficient dissociation. In Case 2, the hydrate dissociation was delayed and marked by multiple fluctuations in water saturation. This intermittent pattern can be attributed to a feedback loop between local hydrate reformation and pore-scale flow obstruction. Insufficient gas replenishment and localized cooling due to endothermic hydrate dissociation caused temporary reductions in decomposition rate. These instabilities indicate that heat transfer and mass availability became rate-limiting steps, particularly when the local permeability was partially impaired by capillary retention or transient blockages. In Case 3, hydrate decomposition exhibited the most delayed and nonlinear behavior. For the first 60 mins, water saturation remained nearly unchanged, suggesting a strong resistance to hydrate breakdown. This can be explained by the combined effects of high initial hydrate saturation, elevated flow pressure, and localized pore-scale overburden, which together favored secondary hydrate formation and flow blockage. Only after a critical pressure drop was reached, leading to mechanical destabilization and pore-space release, did hydrate begin to decompose, reflected by a gradual increase in water saturation. This illustrates a threshold-driven, phase-change-controlled reopening of the flow regime.

In summary, Fig. 3 quantitatively captured the dynamic interplay between hydrate phase transitions, fluid transport, and pore-scale connectivity. The underlying mechanism involved

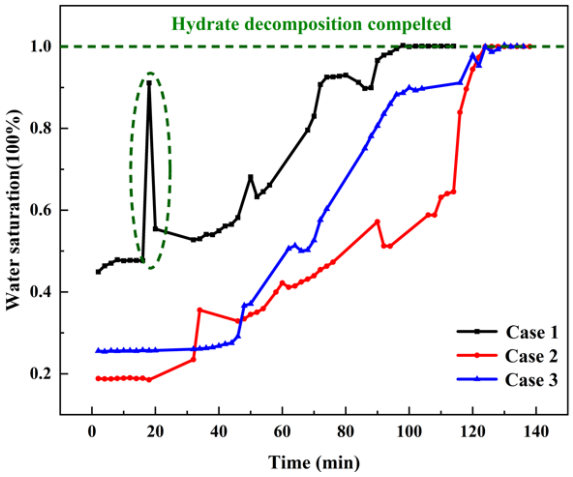

Fig. 3 Variation of water saturation during hydrate phase transition process in Cases 1~3

a strong feedback loop: hydrate decomposition modifies pore structure and flow paths, while evolving flow conditions in turn alter local temperature and pressure fields, either promoting or suppressing further decomposition. This coupling was especially pronounced under high saturation conditions, where small disturbances in pressure or heat supply can tip the system toward temporary blockage or rapid channel reopening.

Understanding this mechanism was essential for accurately predicting hydrate behavior in hydrate-bearing systems, especially those involving depressurization driven decomposition. Although the current findings were based on lab-scale experiments, similar dynamic responses, such as flow intermittency, local blockage, and delayed water release, have also been observed in prior pore-scale investigations [23-25]. These findings suggested that the identified feedback loop may be a fundamental mechanism governing hydrate-flow interactions across scales. Further validation using larger-scale physical models or well-interpreted field test data would be beneficial to confirm its relevance under realistic reservoir conditions.

4 Conclusions

In this study, the coupling mechanism between gas-water two-phase flow and methane hydrate phase transitions was systematically investigated under varying initial hydrate saturations and pressures. The following key conclusions were drawn: (1) At lower hydrate saturation and pressure, the system maintained a stable and continuous two-phase flow regime, enabling efficient and uninterrupted hydrate decomposition. In contrast, higher saturation and pressure conditions delayed the onset of decomposition and triggered intermittent flow blockage, highlighting the sensitivity of flow regimes to thermodynamic conditions. (2) Hydrate phase transitions induced localized structural changes and flow path instabilities, which led to spatially heterogeneous water release and temporary interruptions in flow continuity. This dynamic feedback between decomposition, pore-scale connectivity, and fluid transport plays a critical role in governing hydrate dissociation behavior.

Acknowledgement

The author sincerely thanks all the financial support.

Funding Statement

This project was financially supported by:

The National Natural Science Foundation of China (Grant No. 52406071, 52206076)

China Postdoctoral Science Foundation (2024M750316)

Dalian Science and Technology Talent Innovation Support Program (Grant No. 2024RQ008)

Ph.D. Programs Foundation of Liao Ning (Grant No. 2025-BS-0054, 2023-BS-060)

Dalian Science and Technology Innovation Fund (Grant No. 2023JJ11CG010)

Liao Ning Revitalization Talents Program (Grant No. XLYC2402028)

The Fundamental Research Funds for the Central Universities of China (Grant No. DUT25Z3204, DUT25Z2713, DUT21ZD103).

Author Contributions

The authors confirm their responsibility for the following: study conception and design, data collection, analysis and interpretation of results, and manuscript preparation.

Availability of Data and Materials

None.

Conflicts of Interest

The authors declare that they have no conflicts of interest to report regarding the present study.

References

[1] M. Cha, K. Shin, H. Lee, I.L. Moudrakovski, J.A. Ripmeester, Y. Seo, Kinetics of methane hydrate replacement with carbon dioxide and nitrogen gas mixture using in situ NMR spectroscopy, Environmental Science Technology, 49 (2015) 1964-1971.

[2] B. Castellani, G. Rossetti, S. Tupsakhare, F. Rossi, A. Nicolini, M.J. Castaldi, Simulation of CO2 storage and methane gas production from gas hydrates in a large scale laboratory reactor, Journal of Petroleum Science and Engineering, 147 (2016) 515-527.

[3] J.-C. Feng, Y. Wang, X.-S. Li, G. Li, Z.-Y. Chen, Production behaviors and heat transfer characteristics of methane hydrate dissociation by depressurization in conjunction with warm water stimulation with dual horizontal wells, Energy, 79 (2015) 315-

324.

[4] J.H. Choi, Y. Seol, R. Boswell, R. Juanes, X-ray computed-tomography imaging of gas migration in water-saturated sediments: From capillary invasion to conduit opening, Geophysical Research Letters, 38 (2011) 752-767.

[5] Z.R. Chong, G.A. Pujar, M.J. Yang, P. Linga, Methane hydrate formation in excess water simulating marine locations and the impact of thermal stimulation on energy recovery, Applied Energy, 177 (2016) 409-421.

[6] N. Vedachalam, S. Ramesh, V.B.N. Jyothi, N. Thulasi Prasad, R. Ramesh, D. Sathianarayanan, G.A. Ramadass, M.A. Atmanand, Evaluation of the depressurization based technique for methane hydrates reservoir dissociation in a marine setting, in the Krishna Godavari Basin, east coast of India, Journal of Natural Gas Science and Engineering, 25 (2015) 226-235.

[7] H.R. Sun, J. Chen, X. Ji, G. Karunakaran, B.B. Chen, P.G. Ranjith, Y.C. Song, M.J. Yang, Optimizing CO2 hydrate storage: Dynamics and stability of hydrate caps in submarine sediments, Applied Energy, 376 (2024) 124309.

[8] K. Gajanan, P.G. Ranjith, S.Q. Yang, T. Xu, Advances in research and developments on natural gas hydrate extraction with gas exchange, Renewable and Sustainable Energy Reviews, 190 (2024) 114045.

[9] Y.L. Yuan, T.F. Xu, X. Xin, Y.L. Xia, D. Lu, Multiphase flow behavior of layered methane hydrate reservoir induced by gas production, Geofluids, (2017) 15.

[10] H. Singh, E.M. Myshakin, Y. Seol, A Novel Relative Permeability Model for Gas and Water Flow in Hydrate-Bearing Sediments With Laboratory and Field-Scale Application, Scientific Reports, 10 (2020) 5697.

[11] Y.X. Xia, D. Elsworth, S. Xu, X.Z. Xia, J.C. Cai, C. Lu, Pore-scale gas–water two-phase flow and relative permeability characteristics of disassociated hydrate reservoir, Petroleum Science, 22 (2025) 3344-3356.

[12] M.Y. Wu, H.R. Sun, Q.B. Liu, X. Lv, B.B. Chen, M.J. Yang, Y.C. Song, Enhancing CO2 sequestration safety with hydrate caps: A comparative study of CO2 injection modes and saturation effects, Energy, 320 (2025) 135044.

[13] H.R. Sun, J. Chen, X.H. Yang, P.G. Ranjith, Y.C. Song, B.B. Chen, M.J. Yang, Characterizing methane hydrate phase transitions and multiphase flow behavior in porous media: Insights from low-field nuclear magnetic resonance measurements, International Journal of Heat and Mass Transfer, 253 (2025) 127542.

[14] J.B. Zhang, N.T. Zhang, X.H. Sun, J. Zhong, Z.Y. Wang, L. Hou, S.X. Li, B.J. Sun, Pore-scale investigation on methane hydrate formation and plugging under gas–water flow conditions in a micromodel, Fuel, 333 (2023) 126312.

[15] G.J. Zhao, J.N. Zheng, M.J. Yang, Y.C. Song, Seepage and blockage characteristics of methane hydrate-bearing porous media under different hydrate distribution conditions, Petroleum Science, 11 (2025) 028.

[16] N.T. Zhang, S.X. Li, L.T. Chen, Y. Guo, L. Liu, Study of gas-liquid two-phase flow characteristics in hydrate-bearing sediments, Energy, 290 (2024) 130215.

[17] Y. Seo, S.P. Kang, Inhibition of methane hydrate re-formation in offshore pipelines with a kinetic hydrate inhibitor, Journal of Petroleum Science and Engineering, 89 (2012) 61-66.

[18] X.L. Liu, P.B. Flemings, Dynamic multiphase flow model of hydrate formation in marine sediments, Journal of Geophysical Research, 112 (2007) B03101.

[19] Y.h. Sohn, J. Kim, K. Shin, D. Chang, Y. Seo, Z.M. Aman, E.F. May, Hydrate plug formation risk with varying watercut and inhibitor concentrations, Chemical Engineering Science, 126 (2015) 711-718.

[20] C. Brock, D. Estanga, D.J. Turner, S. Hatscher, L. Ugueto, L.E. Zerpa, E.D. Sloan, C.A. Koh, Development and Field Application of a Flow Pattern

Dependent Gas Hydrate Kinetics and Transportability Model for Transient Multiphase Flow, Energy & Fuels, 39 (2025) 5188-5198.

[21] M. Wu, Wang, G., Zhang, L., Fu, Q., Zhong, L., & Wang, D. , Numerical analysis of phase transition of mining cavity in hydrate solid fluidization exploitation coupled multi-field, Petroleum Science and Technology, (2025) 1-26.

[22] J.L. Cui, K. Li, L.W. Cheng, Q.P. Li, Z.F. Sun, P. Xiao, X.X. Li, G.J. Chen, C.Y. Sun, Experimental investigation on the spatial differences of hydrate dissociation by depressurization in water-saturated methane hydrate reservoirs, Fuel, 292 (2021) 120277.

[23] Sun HR, Chen BB, Zhao GJ, Zhao YC, Y. MJ, Utilization of water-gas flow on natural gas hydrate recovery with different depressurization modes, Fuel, 288 (2021) 119583.

[24] H.R. Sun, B.B. Chen, W.X. Pang, Y.C. Song, M.J. Yang, Investigation on plugging prediction of multiphase flow in natural gas hydrate sediment with different field scales, Fuel, 325 (2022) 124936.

[25] H.R. Sun, B.B. Chen, Z.M. Yang, Y.C. Song, M.J. Yang, Natural gas hydrate accumulation mechanisms considering the multi-phase seepage and exploitation disturbance in porous media, Fuel, 330 (2022).